A Method to Evaluate Total Supply Capability of Distribution Systems Considering Network Reconfiguration and Daily Load Curves

A Method to Evaluate Total Supply Capability of Distribution Systems Considering Network Reconfiguration and Daily Load Curves

Kening Chen, Wenchuan Wu, *Senior Member, IEEE*, Boming Zhang, *Fellow, IEEE*, Sasa Djokic, *Senior Member IEEE*, and Gareth P. Harrison, *Senior Member, IEEE*

***Abstract*—The total supply capability (TSC) is an important index for assessing the reliability of a distribution power system. In this paper, two models to evaluate the TSC are established. In the first, the TSC is acquired with the conditions that all load outages can be restored via network reconfiguration with transformers' *N*-1 contingencies, i.e., that all constraints related to branch thermal ratings and bus-voltage limits can be satisfied following restoration for each *N*-1 contingency. The second model, which is revision of the first, considers the daily load curves for different classes of customers, e.g., residential, commercial and industrial. Both models can be formulated as mixed integer problems with second-order cone programming (MISOCP), which can be solved using commercially available optimization software. Two test systems are used to demonstrate the applicability of the presented models. Numerical results show that the presented model is more accurate than the previously published models. This proposed analytical approach can be applied in a range of network planning studies, e.g., for selecting appropriate ratings of transformers, or for optimal locating of circuit breakers and distributed energy resources.**

***Index Terms* – Total supply capability, distribution power system; N-1 contingency; daily load curves**

I. Nomenclature

Φ_N : Set of all buses, excluding root buses.

Φ_R : Set of root buses.

Φ_{DG} : Set of buses with distributed generation (DG).

N_{node} : Number of all buses, excluding root buses.

N_{trans} : Number of transformers.

N_{time} : Number of all considered time points of a day.

$N(i)$: Set of buses connected to bus *i* by a branch.

B : Set of branches directly connected to a faulted transformer.

$L_{P,i}, L_{Q,i}$: Active and reactive power demands at bus *i*.

f : Scenario in which transformer *f* is faulted.

x_{ij} : State of branch *i-j*; 0 represents disconnected and 1 represents connected branch.

d_{ij} : Direction parameter for branch *i-j*.

$P_{ij,i}$: Active power flow on terminal-*i* of branch *i-j*.

$Q_{ij,i}$: Reactive power flow on terminal-*i* of branch *i-j*.

$L_{P,i}^{DG}, L_{Q,i}^{DG}$: Maximum active and reactive power output of the DG connected to bus *i*.

φ_i : Power factor of the load connected to bus *i*.

$\bar{S}_{ij}$: The power limit for branch *i-j*.

u_i : The voltage magnitude for bus *i*.

U_i^S : The square of the voltage magnitude for bus *i*.

I_{ij} : The current for branch *i-j*.

I_{ij}^S : The square of the current for branch *i-j*.

$\underline{U}_i^S, \bar{U}_i^S$: Lower and upper boundaries for the square of voltage magnitude for bus *i*.

M_0 : A large positive number.

M_{ij} : A relaxation variable of branch *i-j*.

R_{ij}, X_{ij} : The resistance and reactance of branch *i-j*.

S_i : The output apparent power of transformer *i*.

$S_i^{\max}$: The rating of transformer *i*.

t : Time point of a day.

$\alpha(t), \beta(t), \gamma(t)$: Proportions of load values at time *t* with respects to the peak values of aggregate daily load curves for residential, commercial and industrial customers, respectively.

$\bar{L}_{P,i}$: The peak value of daily load curve at bus *i*.

Φ_R, Φ_C, Φ_I : The set of buses where residential, commercial and industrial loads are respectively connected.

$V^f(t)$: The form of variable *V* for scenario *f* (at time point *t*), generally representing x_{ij}, $P_{ij,i}$, $Q_{ij,i}$, etc.

II. Introduction

POWER distribution systems in urban areas are designed as meshed networks, but are typically operated in radial

This work was supported in part by the National Key Basic Research Program of China (Grant 2013CB228206), in part by the National Science Foundation of China (Grant 51477083),in part by the China Scholarship Council.

K. Chen, W. Wu, B. Zhang are with the State Key Laboratory of Power Systems, Department of Electrical Engineering, Tsinghua University, Beijing 100084, China (e-mail: wuwench@tsinghua.edu.cn).

S. Djokic and G. P. Harrison are with the Institute for Energy Systems, School of Engineering, University of Edinburgh, Edinburgh, EH9 3DW, U.K. (e-mail: sasa.djokic@ed.ac.uk; gareth.harrison@ed.ac.uk).

configurations with normally open switches on the tie lines interconnecting ends of radial feeders and on the lines providing connections to alternative supply points [1]. Consequently, after a permanent fault occurs and is isolated by protection system, distribution network operators (DNO) will try to reconfigure the network, in order to maintain continuous power supply to all, or most of the connected loads. The ability of the network to transfer the loads that would be otherwise interrupted to a reconfigured supply point becomes a significant feature, reflecting the overall network reliability performance [2]. It is, therefore, necessary to assess the total supply capability of the considered network in different planning and operation applications by considering supply restoration and load recovery under relevant N-1 system contingencies.

Some early studies reported reduced models to evaluate network supply capability, taking into account only substation power ratings. References [3]-[5] researched load capacity and load recovery, but a proper concept of total supply capability (TSC) had not been proposed until [6] were reported, where transformer contingencies were found to be the most severe and for which TSC should be assessed. Based on this TSC concept, further studies has been conducted: [8] studied impact of load growth and load forecasting based on probability theory; [9] considered power flow when computing TSC and took into account voltage constraints and network losses, making the model more accurate. However, the existing TSC algorithms consider only routings among feeders and transformers, without formulating the detailed network and load connections within a feeder and without taking into account actual load distributions for considered buses. As a result, the reconfiguration capability of the entire distribution system was not exhaustively investigated and the model lacked flexibility to include practical operating conditions.

To improve these aspects of evaluating TSC, an optimization model for distribution network restoration formulated as mixed-integer problem would be required. A description of the radial restrictions was introduced in [10], while [11] and [12] proposed practical optimization methods for distribution system reconfiguration. However, in this work network losses are ignored for branch power flow modeling. Piecewise linear functions were firstly introduced in [13] to formulate distribution network restoration as a mixed-integer linear programming (MILP) model. Similar idea was also raised in [14]. Both of these two works achieved fairly well performance on computational efficiency and optimality. An approximated linear power-flow (LPF) solution was developed for distribution networks [15], in which each load was modelled as a combination of an impedance and a current source. Based on LPF solution, an efficient MILP model was recently developed and the numerical tests show this method has good performance [16]. To hedge the uncertainty of load demand, a robust network reconfiguration method was proposed in [17], in which network reconfiguration was formulated as two-stage robust optimization model incorporated with optimal power flow problem.

Based on the works [11] [12], [18] and [19] proposed an improved restoration algorithm, which is adopted in this paper, accompanied with the idea of using conic relaxation technique from [20]. Regarding the previous works, the main contributions of this paper are:

(1) A second-order cone programming with mixed-integer (MISOCP), considering network losses based on [19] and [20], is established for the analysis of distribution network reconfiguration functionalities.

(2) Based on (1), two improved TSC evaluation models are presented. In the first model, the reconfiguration capability of an entire distribution system, including detailed network within a feeder, are used to assess more accurately the TSC value that satisfy relevant transformers' N-1 contingencies. The second model acknowledges that different types of system loads have different shapes of daily curves [21]- [22]. Accordingly, the presented TSC assessment methodology includes in the analysis non-coincident peak demands and calculates additional supply capacity which would be otherwise underestimated. The consideration of characteristic daily load curves as the modelling constraints also makes the second presented TSC model more realistic.

The remaining part of this paper is organized as follows. In Section III, two TSC evaluation models are introduced: the first one maximizes TSC with transformers' *N*-1 contingencies via network reconfigurations; the second includes constraints related to daily load curves based on the first TSC model. In Section IV, both models are illustrated using simulations to show their performance and effects. Main conclusions are provided in Section V.

III. Algorithm and Methodology

A. TSC Satisfying N-1 Contingencies

This is the first analyzed TSC model, in which all loads interrupted after a permanent fault of a transformer are guaranteed to be restored. Under this assumption, the load supplied by the whole system is maximized by optimizing the required reconfiguration actions for a network with given configuration. The detail model is as follows.

1) The objective is given by:

$$Obj.\quad TSC = \underset{L_{P,i}}{Maximize} \sum_{i\in\Phi_N} L_{P,i}\,. \tag{1}$$

The objective is to maximize the total active power that could be supplied to all loads in the system. For simplification, the power factors of loads are assumed to be constant (0.9 in the following numerical tests), so that the supply of reactive demand is acquired when the active demand at the same bus is confirmed.

2) The constraints are as follows:

$$\begin{cases} x_{ij}^{f} \in \{0,1\}, \sum x_{ij}^{f} = N_{node} \\ x_{ij}^{f} = 0,\ i\text{-}j \in B \end{cases} \tag{2}$$

$$d_{ij} = -d_{ji},\ d_{ij} \in \{1,-1\} \tag{3}$$

$$\begin{cases} \sum_{j\in N(i)} d_{ij}P_{ij,i}^{f} = L_{P,i},\ \sum_{j\in N(i)} d_{ij}Q_{ij,i}^{f} = L_{Q,i} \\ L_{P,i} > 0, \quad L_{Q,i} = \dfrac{\sqrt{1-\varphi_i^2}}{\varphi_i} L_{P,i} \end{cases} \tag{4}$$

$$\begin{cases} -L_{P,i}^{DG} \le \sum_{j\in N(i)} d_{ij}P_{ij,i}^{f} < 0, \\ -L_{Q,i}^{DG} \le \sum_{j\in N(i)} d_{ij}Q_{ij,i}^{f} < 0,\ i \in \Phi_{DG} \end{cases} \tag{5}$$

$$\left(P_{ij,i}^{f}\right)^2 + \left(Q_{ij,i}^{f}\right)^2 \le x_{ij}^{f}\bar{S}_{ij}^2,\ \left(P_{ij,j}^{f}\right)^2 + \left(Q_{ij,j}^{f}\right)^2 \le x_{ij}^{f}\bar{S}_{ij}^2 \tag{6}$$

$$U_i^{S,f} = \left(u_i^{f}\right)^2,\ I_{ij}^{S,f} = \left(I_{ij}^{f}\right)^2 \tag{7}$$

$$d_{ij}\left(U_i^{S,f} - U_j^{S,f}\right) = \left(P_{ij,i}^{f} + P_{ij,j}^{f}\right)R_{ij} + \left(Q_{ij,i}^{f} + Q_{ij,j}^{f}\right)X_{ij} \tag{8}$$

$$\underline{U}_i^{S} \le U_i^{S,f} \le \bar{U}_i^{S} \tag{9}$$

$$I_{ij}^{S,f} = \left[\left(P_{ij,i}^{f}\right)^2 + \left(Q_{ij,i}^{f}\right)^2\right] / U_i^{S,f} \tag{10}$$

$$P_{ij,i}^{f} - P_{ij,j}^{f} = d_{ij}I_{ij}^{S,f}R_{ij},\ Q_{ij,i}^{f} - Q_{ij,j}^{f} = d_{ij}I_{ij}^{S,f}X_{ij} \tag{11}$$

$$\begin{cases} 0 \le I_{ij}^{S,f}U_0^{S} \le \left(S_i^{\max}\right)^2, i \ne f \\ I_{ij}^{S,f} = 0, i = f, and\ i, f \in \Phi_R \end{cases} \tag{12}$$

$$f = 0,1,2,...,N_{trans} \tag{13}$$

Where:

Equation (2) describes the states of branches as Boolean values. For a radial topology, the number of all connected lines is always equal to the number of nodes minus the number of roots. The second row of (2) means that the faulted transformer branch *i-j* is isolated/disconnected for contingency *f*. If a meshed network is analyzed, $\sum x_{ij}^{f} = N_{node}$ should be written as $\sum x_{ij}^{f} = N_{node} + K$, where *K* represents the number of independent loops. Here, $i\text{-}j \in f$ means that the branch *i-j* is connected to the f^{th} transformer.

Variables in (3) describe the positive directions of branches, which are defined arbitrarily before the model is computed. The direction parameters are constant and known before the optimization.

Equation (4) gives power balance restrictions: the power injection of a bus equals to the sum of the power flows of branches connected to this bus. The reactive power injection is known from the active power injection and the corresponding power factor.

Equation (5) describes the power output limitations for distributed generator (DG) buses.

Equations(2), (4) and (5) together provide sufficient conditions for a radial network structure [10].

Equation (6) expresses the thermal rating constraints for each branch.

Equation (7) uses the first degree variables to replace the second degree ones.

The voltage relationship between nodes at two terminals of a connected branch *i-j* can be described by (8). The derivation of (8) can refer to the appendix. However, (8) cannot be used for disconnected branches: two terminals of a disconnected branch should not have voltage relationship described by (8). In such cases, (14) substitutes (8) [11]: when the branch *i-j* is connected, x_{ij}^{f} equals to 1 and $\left(1-x_{ij}^{f}\right)\cdot M_0$ equals to 0; therefore, (14) is equivalent to (8). When the branch *i-j* is disconnected, x_{ij}^{f} equals to 0 and $\left(1-x_{ij}^{f}\right)\cdot M_0$ equals to M_0; therefore, $d_{ij}\left(U_i^{S,f} - U_j^{S,f}\right)$ is within the range of $\left[-M_0, M_0\right]$, meaning that $\left(U_i^{S,f} - U_j^{S,f}\right)$ has no restrictions, because M_0 is large enough.

$$\begin{cases} d_{ij}\left(U_i^{S,f} - U_j^{S,f}\right) \le \left(1-x_{ij}^{f}\right)\cdot M_0 + \\ \quad \left(P_{ij,i}^{f} + P_{ij,j}^{f}\right)R_{ij} + \left(Q_{ij,i}^{f} + Q_{ij,j}^{f}\right)X_{ij} \\ d_{ij}\left(U_i^{S,f} - U_j^{S,f}\right) \ge -\left(1-x_{ij}^{f}\right)\cdot M_0 + \\ \quad \left(P_{ij,i}^{f} + P_{ij,j}^{f}\right)R_{ij} + \left(Q_{ij,i}^{f} + Q_{ij,j}^{f}\right)X_{ij} \end{cases} \tag{14}$$

Equation (9) restricts the node voltages within the lower and upper boundaries, which can be defined by DNO.

Equation (10) is the branch current expression.

Equation (11) gives the expression of active and reactive power losses of a branch.

Equation (12) describes the rating constraints for transformers; if a transformer is faulted and the fault is isolated in one of the considered scenarios, that transformer will have 0 rating. In (12), U_0^{S} is the square of root voltage and is regarded as a constant value, assuming that voltages are controlled at these root buses.

Equation (13) describes that there are, in total, N_{trans}+1 scenarios, where N_{trans} scenarios represent faults of individual transformers, with one additional scenario representing normal state of the system, i.e., none of the transformers is faulted, given by "*f=0*".

The product of different variables in (10) makes the model unsolvable. To resolve that problem, (10) can be substituted by (15) (16) using SOCP relaxation [20]:

$$Obj.\ \text{Minimize} \sum_{f}\sum_{ij} R_{ij}I_{ij}^{S,f} \tag{15}$$

$$s.t.\ \left\| \begin{matrix} 2P_{ij,i}^{f} \\ 2Q_{ij,i}^{f} \\ I_{ij}^{S,f} - U_i^{S,f} \end{matrix} \right\|_2 \le I_{ij}^{S,f} + U_i^{S,f} \tag{16}$$

This is a classical SOCP problem, where network losses are minimized by (15).

This SOCP relaxation technique can be used to convexify the TSC programming model, where the revised model can be formulated as:

$$Obj.\ \underset{L_{P,i}}{Maximize}\left(\sum_{i\in\Phi_N} L_{P,i} - \phi\sum_{f}\sum_{ij} R_{ij}I_{ij}^{S,f}\right) \tag{17}$$

$$s.t. \qquad (2)\text{-}(7),(9),(11)\text{-}(14),(16)$$

The first term in (17) is TSC, while the second term is the penalty with a weighted network losses form, with ϕ as the weighting coefficient. This model is a MISOCP model and can

be solved by available commercial software packages, such as CPLEX. As numerical tests in Section IV confirm, the application of relaxation method [20] has acceptable accuracy for the proposed TSC model.

The above constraints are used for solving power flows, based on the corresponding network configurations. For any transformer fault case, all loads in the system should be supplied without violating any of the operating constraints. There are in total N_{trans}+1 sets of system variables and constraints with the same objective, which is to maximize the total load that can be supplied in the considered network. In the model, detailed power flow solution constraints are considered, in order to assess the overall network capability to supply the system load by applying optimal network reconfigurations.

B. TSC Considering both N-1 Contingencies and Daily Load Curves

In Section III.A, loads/demands at buses $L_{P,i}$ were considered to be independent variables, so that each load is represented with only one value: peak demand at that bus. In reality, however, the load will change at different times of a day, rather than to stay constant. The same class of loads will have similar shape of daily load curves, representing similar temporal variations of demands, which may be different in the actual amounts. As the differences in shapes of load curves among different classes of customers are evident, it is necessary to take assumed or known daily load curves into account for a more accurate assessment in the TSC model.

Without any loss of generality, three parameters are introduced, $\alpha(t)$, $\beta(t)$ and $\gamma(t)$, representing the proportions of the corresponding peak demands at time t of a day for residential, commercial and industrial load classes respectively. Therefore, the value of the load/demand at bus i at time t can be represented as follows:

$$\begin{cases} L_{P,i}(t) = \alpha_P(t) \cdot \bar{L}_{P,i}, \ i \in \Phi_R \\ L_{P,i}(t) = \beta_P(t) \cdot \bar{L}_{P,i}, \ i \in \Phi_C \\ L_{P,i}(t) = \gamma_P(t) \cdot \bar{L}_{P,i}, \ i \in \Phi_I \end{cases} \tag{18}$$

In (18), $\bar{L}_{P,i}$ are unknown variables which should be optimized. Contribution of the residential loads to the total demands at bus i at time t is expressed as a proportion $\alpha(t)$of its peak daily value $\bar{L}_{P,i}$; similar approach is used for commercial and industrial loads. Parameters $\alpha(t)$, $\beta(t)$ and $\gamma(t)$ can be acquired from historical data analysis and in this paper, they are estimated from the typical daily load curves from [21], by computing the ratio of load at time "t" to the corresponding daily peak load. Further assumption is made that there is only one load class at each bus, i.e., there are no mixes of three considered load classes at any bus, which is often the case in practice.

The full daily load curves contain 48 load points (each 30min) and cannot be applied directly in the calculation due to complexity. Instead, these curves have been simplified by selecting five characteristic points from the original curves, as shown in Fig.1. For instance, value of $\alpha(t=12:00)=0.6$ in Fig.1, means that residential load contribution in the computation should be 60% of its peak load at 12:00. Similar explanations can be made for $\beta(t=5:00)=0.6$ and $\gamma(t=8:00)=0.85$. The corresponding peak load times for residential, commercial and industrial load classes are at 18:00, 12:00, 12:00, respectively, when α, β *and* γ are equal to 1.

The more time points are selected per day and the more load classes are considered (if present in the considered network), the more accurate result will be obtained, but this will also result in heavier computational burden. To make the computation feasible, we considered only five time points during a day: at 05:00, 08:00, 12:00, 18:00 and 00:00 hours, which are assumed to be representative of the actual shape of each daily load curve (these time points are selected to include the main turning points on the original daily load curves for different customer classes).

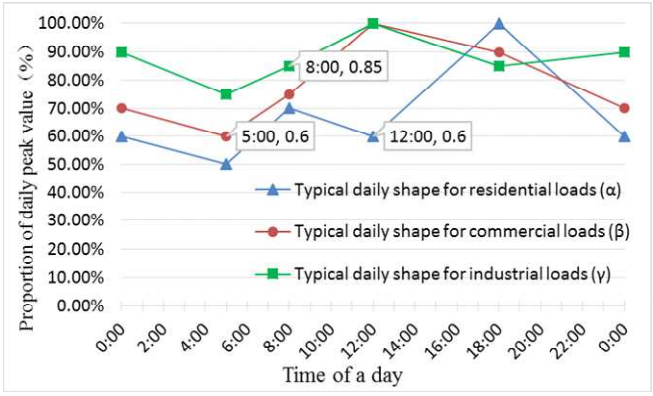

Fig. 1. Simplified daily load curves for residential, commercial and industrial loads, normalized to the daily peak load for that load class.

The variables introduced in Section III.A should be extended as follows:

$$\begin{cases} \left(P_{ij,i}^f, Q_{ij,i}^f\right) \rightarrow \left(P_{ij,i}^f(t), Q_{ij,i}^f(t)\right) \\ x_{ij}^f \rightarrow x_{ij}^f(t) \\ U_i^{S,f} \rightarrow U_i^{S,f}(t) \\ M_{ij}^f \rightarrow M_{ij}^f(t) \\ S_i^f \rightarrow S_i^f(t) \end{cases} \tag{19}$$

The objective function also changes:

$$\begin{aligned} Obj.\,TSC: \max_t \{ \max_{\bar{L}_P} [& \sum_{i \in \Phi_R} \left(\alpha_{P,i}(t) \cdot \bar{L}_{P,i}\right) + \\ & \sum_{i \in \Phi_C} \left(\beta_{P,i}(t) \cdot \bar{L}_{P,i}\right) + \sum_{i \in \Phi_I} \left(\gamma_{P,i}(t) \cdot \bar{L}_{P,i}\right)] \} \end{aligned} \tag{20}$$

This new objective in (20) maximizes the peak of the total load supplied to the three different classes of customers during a day in the system, and is, accordingly, again considered as the TSC for the system. Before this optimization problem is solved, it is not known at what time of a day the maximum demand in the considered network will occur. For each selected time point in a day, the total load will be maximized at N_{time} time points of a day respectively. The peak/maximum demand can be acquired by choosing the maximum of the N_{time}

solutions to (20).

The total number of variables and constraints is significantly larger than for the TSC model described in Section III.A with:

$$\begin{cases} f = 0,1,2,...,N_{trans} \\ t = 1,2,...,N_{time} \end{cases} \quad (21)$$

There are, in total, $(N_{trans}+1)\cdot N_{time}$ sets of variables and scenarios in this model; i.e.,

$$(f,t): \begin{bmatrix} (f_0,t_1), & (f_0,t_2), & \dots, & (f_0,t_{N_{time}}) \\ (f_1,t_1), & (f_1,t_2), & \dots, & (f_1,t_{N_{time}}) \\ (f_2,t_1), & (f_2,t_2), & \dots, & (f_2,t_{N_{time}}) \\ \dots & & & \\ (f_{N_{trans}},t_1), & (f_{N_{trans}},t_2), & \dots, & (f_{N_{trans}},t_{N_{time}}) \end{bmatrix} \quad (22)$$

Both of the TSC models described in this and previous section are MIQCP problems, which can be solved by commercial software packages (e.g. CPLEX).

IV. Simulations and Analysis

A. Six-Feeder Test System Introduction

The test system is shown in Fig. 2. It combines six standard IEEE 33-bus networks, as shown in Fig. 3.

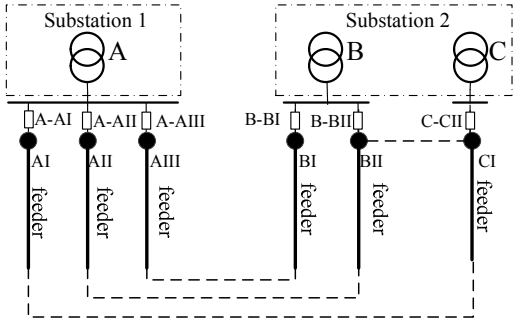

Fig. 2. The "Six-feeder" test system used for the analysis (a combination of six IEEE 33-Bus networks, Fig. 3).

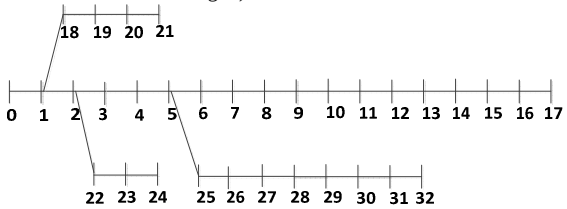

Fig. 3. The IEEE 33-Bus test distribution network, used for building the test system used for the analysis in Fig. 2.

There are three transformers in Fig. 2: A, B and C. Transformers B and C are in the same substation, while A is in another. They also have different numbers of feeders connected: three feeders (AI, AII and AIII) are connected to transformer A, two (BI and BII) to transformer B and one (CI) to transformer C, are all marked by bold lines in Fig. 2. Each feeder represents a standard IEEE 33-Bus test network, as shown in Fig. 3. The dotted lines in Fig. 2 represent normally disconnected tie lines between the feeders. The bold points are direct connections to transformers, i.e., feeder roots, marked as "bus 0" in Fig.3.

As shown in Fig.2, the six feeders connect to their transformers via breakers A-AII, A-AIII, B-BI, B-BII, C-CI respectively. The normally disconnected link branches among substations include AI.17-CI.17, AII.17-BII.17, AIII.17-BI.17. Where, the number following dot is the original node number inside a feeder. For example, AI.17 represents the 17th node in feeder AI .

The following assumptions are used during the analysis of test network from Fig. 2 and Fig. 3:

1) All buses are PQ buses with a constant power factor 0.9.
2) The voltages at root buses are 1.1 p.u., the lower boundary for bus voltages is 0.9 p.u. in most cases, the branch thermal limit is set to be 7 MVA.
3) All loads are constant power loads, so that voltage variations during reconfiguration will not impact P and Q demands at these buses.
4) The additional assumptions about DER, breakers and link branches of the feeders will be discussed in corresponding simulations.

B. Impact of Weight of the Relaxing Objective to TSC and the accuracy of SOCP Relaxation

Numerical tests are made based on the system in Fig.2, using the optimization model introduced in section III.A, with a 0 valued f (which means a normal state scenario).

Fig.4 shows when the weight coefficient ϕ is within a range ([0.01,10] in this case), the TSC will almost not be affected by the penalty term (weighted network loss in (17)) and the network loss also keeps constant. That is to say, the final decision for variables x_{ij} and $L_{P,i}$ keep unchanged when ϕ is below a threshold. However, if ϕ is above the threshold, the TSC and network losses both decrease. This is because the value of weighted network loss is comparable to TSC with large ϕ and the objective (17) is significantly affected by the weighted network loss.

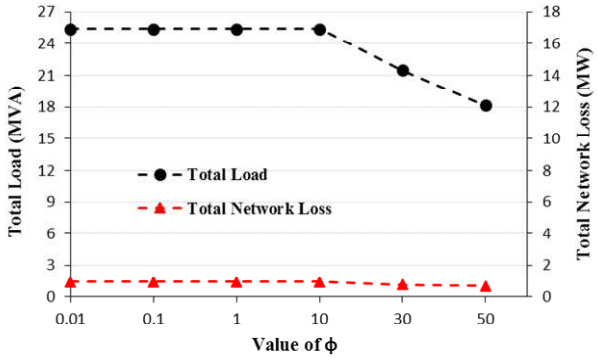

Fig. 4. Effect of weight to the value of calculated TSC and corresponding network loss

To evaluate the accuracy of the SOCP relaxation (16), a gap (relaxation error) is defined as

$$Gap = \max_{ij} \left| \sqrt{I_{ij,i}^{S}} - \sqrt{\frac{(P_{ij,i})^2 + (Q_{ij,i})^2}{U_i^S}} \right| \quad (23)$$

If the relaxation error (gap value) is zero or relatively small, the relaxation technique is practical for this model.

The relationship curve between the gap and weight coefficient ϕ is shown in Fig.5. From Fig.5, we can see that relaxation error is kept relatively small when ϕ changes (the maximum relaxation error among these tests is within 0.5 A, and will be much smaller when ϕ is larger than 1, meanwhile the current of a branch could be up to 110 Ampere on average), i.e. the SOCP relaxation has quite acceptable accuracy for this problem.

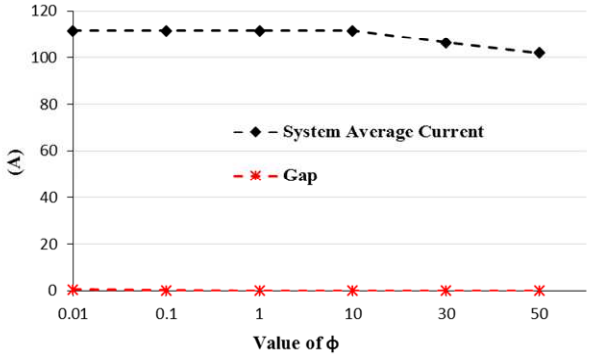

Fig. 5. Effect of weight coefficient ϕ to relaxation error (Gap)

From the tests above, we can conclude that the relaxed SOCP method can accurately calculate TSC when an approximately value (it is within a relatively large range) is chosen for ϕ.

C. Results for TSC satisfying N-1 Contingencies

In this section, only N-1 transformer contingencies are considered for computing TSC value, and the Six-Feeder Test System is used.

(1) Effect of network reconfiguration on TSC

In this simulation, the lower voltage boundary is set at 0.9 p.u. and the rating of each transformer is set to be 9 MVA.

The calculated TSC value satisfying all N-1 transformer contingencies is 14.07 MVA. That TSC value is much lower than the sum of transformer ratings, or sum of feeder limits, when actual operational constraints are considered. This system can take totally 14.07 MVA loads if N-1 is requested. Most amount of load is mainly distributed at buses of: bus 1 of AIII (1.10 MVA), bus 1 of BI (1.10 MVA), bus 1 of BII (4.21 MVA), bus 12 of BII (1.69 MVA), bus 1 of CI (2.75 MVA), bus 12 of CI (1.69 MVA), etc.. The load distribution results show which locations are better to take heavy loads for TSC satisfying N-1 contingencies.

All of the loads are able to get restored after any transformer contingency and keep their amount. For different contingencies, different branch operations are listed in Table I.

TABLE I

Branch States under *N*-1 and Normal Scenarios

Fault	Disconnected Branches (The other branches not listed in this table are connected)
Transformer A	A-AI, A-AII, A-AIII, and BII.17-CI.17
Transformer B	B-BI, B-BII, and BII.11-BII.12, CI.11-CI.12
Transformer C	C-CI, AIII.11-AIII.12, BII.11-BII.12, CI.11-CI.12
No Fault	AI.11-AI.12, AII.11-AII.12, BI.11-BI.12, BII.17-CI.17

Fig.6 shows how the breakers within feeders will affect the result of TSC.

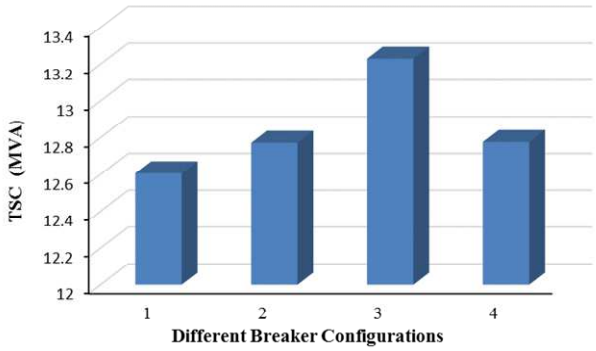

Fig. 6. Different TSC values with different breaker configurations (lower voltage boundary is 0.94 p.u. and transformers' ratings are 9 MVA)

Four different breaker configurations are designed, and corresponding TSCs are illustrated in Fig.6:

Case 1: no breakers within any feeder;

Case 2: breakers located at 11-12 for each feeder (same configuration as tests in Table I);

Case 3: breakers located at 11-12 for each feeder and 17-32 for feeder CI;

Case 4: breakers located at 4-5 for each feeder and 24-28 for feeder CI.

By comparing results for Cases 1, 2 and 3, we can see that setting more reconfiguration options will increase TSC, because more breakers and connections bring more possible routings to avoid violating constraints. Case 3 and 4 shows that different deployment of breakers and link branches lead to different TSCs, which is important for network planning.

(2) Effects of voltage bounds and transformer ratings on TSC

In addition to network reconfiguration capabilities, the other two main factors that will affect the TSC are voltage constraints (lower boundary) and transformer ratings.

Fig. 7 shows the effects of the voltage constraints on the TSC value, where all transformer ratings are set to be 7 MVA, showing that the TSC values are decreasing when the lower bound for voltage is higher than 0.86 p.u. It also means that when the lower boundary of voltage is smaller than 0.86 p.u., the key factor in determining TSC value is not voltage constraints, but transformer ratings.

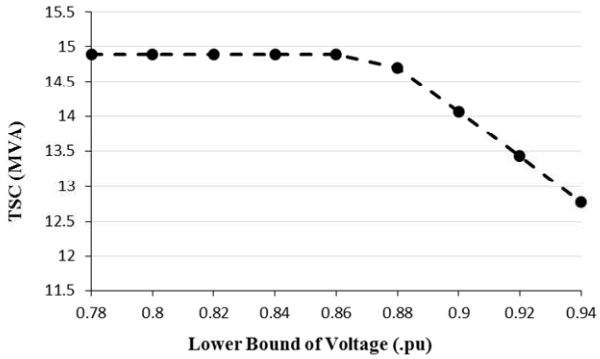

Fig. 7. The effects of voltage constraint (lower boundary) on TSC value with a constant transformer rating of 7 MVA.

Fig.8 shows the effects of the transformer ratings on the TSC. Assessed value of TSC is increasing until the rating reaches 8.9 MVA. Therefore, further increasing the ratings of transformers will be inefficient for the applied voltage limits, demonstrating the TSC cannot always be increased by raising transformer ratings.

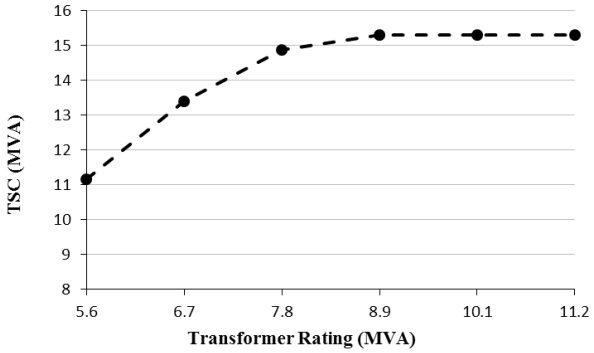

Fig. 8. The effects of transformer ratings on TSC when the lower boundary of voltage is set at 0.9 p.u.

The combined effects of voltage lower boundary and transformer rating on the assessed TSC values are illustrated in Fig.9. This figure demonstrates that TSC analysis can provide guidance for transformer design in distribution system planning, according to the corresponding voltage constraints, in order to optimally utilize the capacity of transformers. Also, when the ratings of transformers are limited, voltage regulators can be applied to achieve a better supply capability of a system, and this TSC analysis will be important clues for the regulation. In our model, voltage regulations can be treated as different configuration of voltage at feeder roots.

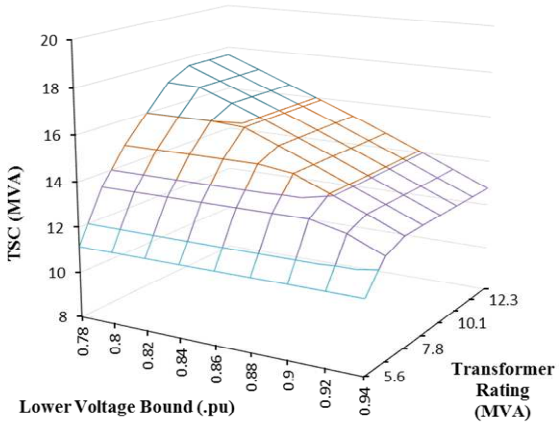

Fig. 9 Combined effects of voltage constraints (lower boundary) and transformer ratings on the TSC value.

(3) Effects of distributed generators on TSC

As described in Sub-Section IV.C (2), TSC values are mainly affected by voltage limits. The flows of both active and reactive powers will impact voltage drops and profiles. Active and reactive output from distributed generation (DG), if present in the network, may possibly relieve voltage problems, provided that the DG are at suitable locations.

In the considered system, buses with low loads, which contribute little to the TSC, may be chosen as DG buses. In the test network, these are buses 3, 6, 9 of A1, and bus 6 of C1, which are chosen to locate DG, corresponding to locations 1, 2, 3 and 4 respectively in Fig. 10. Assuming that the active power output of each DG in the range [0,0.5] MW and the reactive power output [0,0.25] MVar.

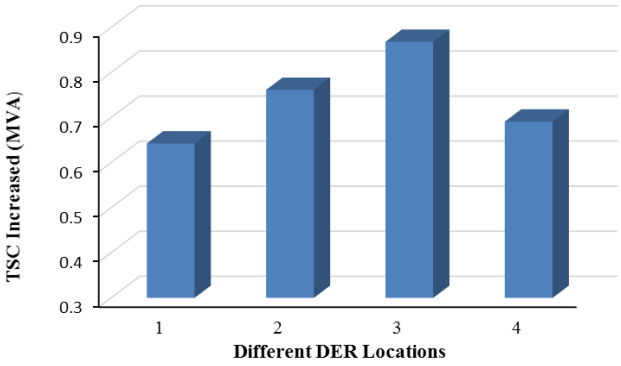

Fig. 10. TSC increase by DG located at different buses (for lower voltage boundary of 0.9pu and transformer ratings of 9 MVA)..

It could be seen from Fig.10 that penetration of DG at any location is contributing to an increase of TSC. In all cases, the increase of TSC is greater than a DG maximum output, because DG contributes not only by installed power, but also by improving network voltage profiles.

Among all these cases, DG at bus 9 of A1 (Case 3 of Fig.10) provides most significant TSC gains. The network is always changing under different N-1 scenarios. If a DG is far away from the roots in most reconfigurations, it will provide stronger voltage support than the ones closer to roots. The best DG location for TSC improvement could not be simply

acquired, unless the TSC tests are simulated and analyzed. Generally, the numerical approach of calculating the TSC provides insight into the optimal locations for DG, which can also be a reference for system planners to decide where to locate DG.

D. TSC Considering both N-1 and daily load curves

To use the model in Section III.B, assumptions are made previously that a third of all buses are randomly chosen as residential loads, a third as commercial loads and a third as industrial loads. Still the transformer ratings are all 9 MVA and lower voltage boundary is set to 0.9 p.u. in this test.

At the five time points during a day, the model maximizes the total load of the system. The results are 13.36 MVA at 00:00, 11.16 MVA at 05:00, 13.32 MVA at 08:00, 15.02MVA at 12:00 and 15.04 MVA at 18:00. The TSC is 15.04 MVA, and the relevant curve is shown in Fig. 11. The peak occurred at 18:00 can be considered as the TSC of the system.

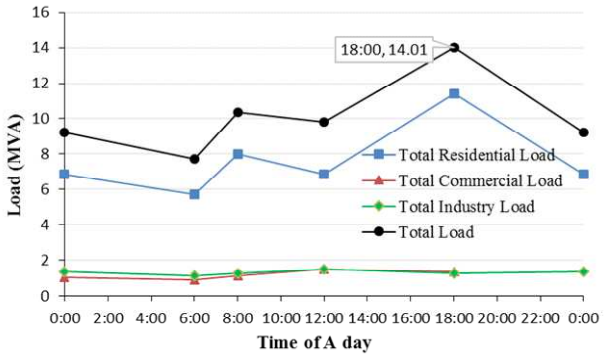

Fig.11. Total load curve. The black curve shows the total system daily load curve under TSC conditions. The residential load is shown in blue, the commercial load in red, and the industrial load in green.

According to the applied TSC model, the peak residential load is 11.43 MVA, the peak commercial load is 1.48 MVA, and the peak industrial load is 1.48 MVA, which in principal gives a total load of 14.39 MVA; however, this can be supplied by a system with a capability of 14.01 MVA, because these peaks occur at different times of day. Exactly this feature is incorporated in the presented TSC method, which considers daily load curves of different customer classes.

E. TSC results compared with the method in [7]

In this section, a test system introduced in [7] is adopted to compare the existing methods and the method presented in this paper. In addition to tie lines between feeders, branches 31-37, 38-44 and 15-16 are also assumed operational, while the lower voltage boundary is set to 0.9 p.u..

The TSC acquired by different models are listed in Table II.

TABLE II
TSC values by different models.

Model Adopted	TSC (MVA)
Model in Refs. [6] and [7].	161.70
Model in Section III.A without the operational branches within Feeders.	97.86
Model in Section III.A with operational branches within Feeders.	106.85
Model in Section III.B	104.04

The total transformer capacity is 269MVA. Each transformer in the system takes one or two feeders and the capacity of transformers are mostly larger than the sum of their feeder capacities, except for T1. Using the model described in Section III.A, the TSC for the test system is 106.85 and 97.86 MVA with and without the ability to reconfigure within feeders respectively. Compared with the value of 161.70 MVA without imposing power-flow constraints, the TSC decreased considerably, which is attributable primarily to satisfying voltage constraints. Therefore, this model, which considers the power flow, will provide a more accurate and realistic TSC for the considered system. In addition, the difference between the models with and without network reconfiguration is also obvious. It can be seen that power flow restrictions may cause a lower TSC, and operational branch considerations may result in a larger TSC, so both aspects will improve the accuracy to compute TSC.

F. Computing Efficiency

The TSC model in this paper is programmed using C++, and the optimizations are solved by CPLEX software package which can be embedded in VS2008. This work has been done in Windows 7 environment (32), with CPU of Intel Core i3, 4G RAM and 2.53GHz frequency.

For the Six-Feeder test system, one TSC simulation considering N-1 scenarios involves 4 scenarios (3 contingency scenarios and 1 normal scenario); while load shapes are considered, the total scenarios increases to 20. The computation time for the two situations takes about 10 seconds and 2 minutes respectively.

For the system introduced in [7], one simulation considering N-1 involves 9 scenarios, and there are about 500 buses, taking about 20 seconds on average for one case. When load shapes are considered, number of scenarios increases to 45, requiring around 30 minutes CPU time. The computing time will possibly increase significantly when the number of binary variables is large. However, a large distribution system can be divided into several isolated areas within an acceptable scale and can be calculated separately. Above all, the method proposed in this paper is mainly for planning use rather than online application.

V. Conclusion

In this paper, the assessment of distribution network TSC value is modeled as a MISOCP optimization problem. Using this model, two significant improvements can be realized compared to the existing methods:

1) The reconfiguration capability of an entire distribution power system, including not only routings and tie lines between feeders, but also detailed configuration within feeders, can be included in computation of the TSC. Moreover, how much load each bus is supposed to take to achieve larger TSC

satisfying N-1 can also be obtained.

2) Daily load curves for different classes of customers are considered in the analysis. By taking advantage of non-coincident load peaks, TSC can be more appropriately evaluated.

The two improvements for TSC calculation effectively make the TSC analysis more accurate and practical. Thus, the TSC results can be used as better guidelines for distribution network planning and configuration purposes, like load planning, breaker and DG locating, transformer rating designing and so on. In the future work, load curves at different time scales providing more flexibility in the model will be studied.

APPENDIX

The relationship between the voltages on two terminals of a branch can be illustrated as Fig. A-1.

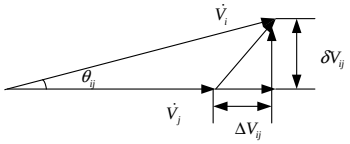

Fig. A-1 The relationship between the voltages on two terminals of a branch

Define $\Delta V_{ij} = \left(P_i R_{ij} + Q_i X_{ij}\right)/V_i$, and $\delta V_{ij} = \left(P_i X_{ij} - Q_i R_{ij}\right)/V_i$. δV_{ij} can be ignored, because θ_{ij} (the phase angle difference between two adjacent nodes) is very small.

From two terminals of a branch i-j, we have

$$\begin{cases} V_i = V_j + \dfrac{P_j R_{ij} + Q_j X_{ij}}{V_j} \\ V_j = V_i - \dfrac{P_i R_{ij} + Q_i X_{ij}}{V_i} \end{cases} \quad \text{(A-1)}$$

(A-1) can be rearranged as

$$\begin{cases} V_i V_j = V_j^2 + P_j R_{ij} + Q_j X_{ij} \\ V_i V_j = V_i^2 - (P_i R_{ij} + Q_i X_{ij}) \end{cases} \quad \text{(A-2)}$$

From (A-2), we can get

$$V_i^2 - V_j^2 = U_i - U_j = (P_i + P_j)R_{ij} + (Q_i + Q_j)X_{ij} \quad \text{(A-3)}$$

Where (A-3) is same with equation (8).

VI. REFERENCES

[1] W. H. Kersting. *Distribution system modeling and analysis*. New Mexico: New Mexico State University Press, pp. 2-9, 2011.

[2] M. R. Kleinberg, K. Miu, H. Chiang, "Improving service restoration of power distribution systems through load curtailment of in-service customers," *IEEE Trans. Power Syst*, vol. 26, no. 3, pp. 1110-1117, Aug. 2011.

[3] N. M. Karen, H. Chiang., "Electric distribution system load capability: problem formulation, solution algorithm, and numerical results," *IEEE Trans. Power Del*, vol. 15, no. 1, pp. 436-442, Jan. 2000.

[4] B. Venkatesh, R. Ranjan, H.B. Gooi, "Optimal reconfiguration of radial distribution systems to maximize loadability," *IEEE Trans. Power Syst*, vol. 19, no. 1, pp. 260-266, Feb. 2004.

[5] Y. Deng, L. Cai, Y. Ni, "Algorithm for improving the restorability of power supply in distribution systems," *IEEE Trans. Power Del*, vol. 18, no. 4, pp. 1497-1502, Oct. 2003.

[6] J. Xiao, F. Li, W. Gu, et al, "Total supply capability and its extended indices for distribution systems: definition, model, calculation and application," *IET Gen., Transm., Distrib.*, vol. 5, no. 8, pp. 869-876, Aug. 2011.

[7] J. Xiao, C. Zhou, P. Zhang, "Study on weak link for distribution network based on total supply capability," in *7th IEEE Int. Power Elect. Motion Control Conf.* , Harbin, China, pp: 1469-1472, Jun. 2012.

[8] Z. Wang, S. Wu, W. Liu, et al, "Total supply capability for city distribution systems based on the probability load growth," in *Innov. Smart Grid Tech. Conf.*, pp. 354-359, May. 2014.

[9] J. Xiao, S. Liu, Z. Li, et al, "Model of Total Supply Capability for Distribution Network Based on Power Flow Calculation," *Proceedings of the CSEE*, vol. 34, no. 31, pp. 5516-5524, Nov. 2014.

[10] M. Lavorao, J. F. Franco, M. J. Rider, et al, "Imposing radiality constraints in distribution system optimization problems," *IEEE Trans. Power Syst*, vol. 27, no. 1, pp. 172-180, Feb. 2012.

[11] J. A. Taylor, F. S. Hover, "Convex models of distribution system reconfiguration," *IEEE Trans. Power Syst*, vol. 27, no. 3, pp. 1407–1413, Aug. 2012.

[12] R. A. Jabr, R. Singh, B. C. Pal, "Minimum Loss Network Reconfiguration Using Mixed-Integer Convex Programming," *IEEE Trans. Power Syst*, vol. 27, no.2, pp. 1106-1115, May. 2012.

[13] A. Borghetti, "A Mixed-Integer Linear Programming Approach for the Computation of the Minimum-Losses Radial Configuration of Electrical Distribution Networks," *IEEE Trans. Power Syst*, vol.27, no.3, pp.1264-1273, Aug. 2012.

[14] J. F. Franco, M. J. Rider, M. Lavorato and R. Romero, "A Mixed-Integer LP Model for the Reconfiguration of Radial Electric Distribution Systems Considering Distributed Generation," *Electric Power Systems Research*, vol. 97, pp. 51-60, Apr. 2013.

[15] J. R. Martí, H. Ahmadi and L. Bashualdo, "Linear Power-Flow Formulation Based on a Voltage-Dependent Load Model," *IEEE Trans. Power Del*,vol. 28, no. 3, pp.1682-1690, July. 2013

[16] H. Ahmadi and J. R. Martí, "Linear Current Flow Equations With Application to Distribution Systems Reconfiguration," *IEEE Trans. Power Syst*, In press.

[17] C. Lee, C. Liu, S. Mehrotra and Z. Bie, "Robust Distribution Network Reconfiguration," *IEEE Trans. Smart Grid*, vol. 6, no. 2, pp. 836–842, Mar. 2015.

[18] K. Chen, W. Wu, B. Zhang, et al, "Security evaluation for distribution power system using improved MIQCP based restoration strategy," in *Innov. Smart Grid Tech. Conf.*, Washington DC, US, pp. 1-5, Feb. 2014.

[19] K. Chen, W. Wu, B. Zhang, et al, "Robust Restoration Decision-Making Model for Distribution Networks Based on Information Gap Decision Theory," *IEEE Trans. Smart Grid*, vol. 6, no. 2, pp. 587-597, March. 2015.

[20] M. Farivar, H. Steven, "Branch flow model: relaxations and convexification (part I)," *IEEE Trans. Power Syst.*, Apr. 2013.

[21] I. H. Gil, B. Hayes, A. Collin, et al, "Distribution network equivalents for reliability analysis. Part 1: Aggregation methodology," in *4th IEEE PES Innov. Smart Grid Tech. Conf.*, Copenhagen, Denmark, pp. 1-5, Oct. 2013.

[22] M. S. Tsai, "Development of an object-oriented service restoration expert system with load variations," *IEEE Trans. Power Syst*, vol. 23, no. 1, pp. 219-225, Feb. 2008.

BIOGRAPHIES

Kening Chen received the B.S. degree in Electrical Engineering Department, Southwest Jiaotong University in 2009, and the Ph.D. degree in electrical engineering from Tsinghua University, Beijing, China, in 2015. He is currently an engineer of State Grid Energy Research Institute, Beijing, China. His research interests include active distribution network security analysis and restoration.

Wenchuan Wu (SM'14) received the B.S., M.S., and Ph.D. degrees from the Electrical Engineering Department, Tsinghua University, Beijing, China. He is currently a Professor in the Department of Electrical Engineering of Tsinghua University. His research interests include Energy Management System，active

distribution networks management and autonomous control， renewable energy generation operation and control，hybrid real-time simulation for AC/DC power systems.

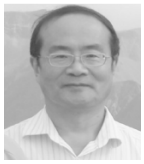

Boming Zhang (SM'95–F'10) received the Ph.D. degree in electrical engineering from Tsinghua University, Beijing, China, in 1985. Since 1985, he has been with the Electrical Engineering Department, Tsinghua University, for teaching and research and promoted to a Professor in 1993. His interest is in power system analysis and control, especially in the EMS advanced applications in the Electric Power Control Center (EPCC). He has published more than 300 academic papers and implemented more than 60 EMS/DTS systems in China. He is now a steering member of CIGRE China State Committee and of the International Workshop of EPCC.

Sasa Djokic (M'05, SM'11) received Dipl. Ing. and M. Sc. degrees in electrical engineering from the University of Nis, Nis, Serbia, and Ph. D. degree in the same area from the University of Manchester Institute of Science and Technology (UMIST), Manchester, United Kingdom. Currently, he is a Reader in the School of Engineering at the University of Edinburgh, Edinburgh, Scotland, United Kingdom.

Gareth P. Harrison (M'02–SM'14) is Bert Whittington Chair of Electrical Power Engineering at the University of Edinburgh, U.K. His current research interests include network integration of renewable generation and analysis of the impact of climate change on the electricity industry.

Prof. Harrison is a Chartered Engineer and member of the IET.